| | | |
|---|---|---|
| 1. Report No.<br>FHWA/TX-08/0-5310-2 | 2. Government Accession No. | 3. Recipient's Catalog No. |
| 4. Title and Subtitle<br>Feasibility Study of Scanning Laser Systems for Measuring Seal Coat Quality | | 5. Report Date<br>September 2007<br>6. Performing Organization Code |
| 7. Author(s)<br>Richard Liu, Wei Sun, Yuanhang Chen, Pankaj Chopra,Yu Cai, Jing Li, Wei Ren and Xuemin Chen | | 8. Performing Organization Report No.<br>Report 0-5310-1 |
| 9. Performing Organization Name and Address<br>Department of Electrical and Computer Engineering<br>University of Houston<br>4800 Calhoun Rd.<br>Houston, TX 77204-4005 | | 10. Work Unit No.<br>11. Contract or Grant No.<br>Project 0-5310 |
| 12. Sponsoring Agency Name and Address<br>Texas Department of Transportation<br>Research and Technology Implementation Office<br>P.O. Box 5080<br>Austin, TX 78763-5080 | | 13. Type of Report and Period Covered<br>Technical Report<br>Sep. 1, 2006 – Aug. 31, 2007<br>14. Sponsoring Agency Code |

15. Supplementary Notes
Project performed in cooperation with the Texas Department of Transportation and the Federal Highway Administration.
URL: http://subsurface.ee.uh.edu/documents/0-5239.pdf

16. Abstract:

In this project the researchers developed a methodology, two hardware systems, and software to evaluate sealcoat quality at highway speed. The methodology is based on mean profile depth (MPD) measured by high speed laser devices. The two hardware systems are texture laser device and scanning laser device. A high-speed texture laser and a 3-D scanning laser system based on auto-synchronized scanning technology are developed in this project. A mean profile depth algorithm based on ASTM standard has been developed and embedded into both point laser and scanning laser devices. The two different devices are mounted on a measurement van and field-tested in pavement sections in San Antonio, Texas. The results of these devices are compared with the MPD value measured by outflow meter. The results are proved to be accurate and can be used in a high-speed measurement in harsh environment. A criterion of automatically identifying a pavement section for flushing, shelling or normal surface conditions is also developed using the field data from both devices. This project is jointly performed by UH and UTSA. UH is responsible for hardware, software and field tests of the laser devices, while UTSA is responsible for identifying test sections and perform CMT and outflow meter measurements.

| | | | |
|---|---|---|---|
| 17. Key Words<br>MPD, ASTM standard, normal, flushing, shelled, criteria. | 18. Distribution Statement<br>No restrictions. This document is available to the public through National Technical Information Service, Springfield, Virginia, 22161, www.ntis.gov | | |
| 19. Security Classif. (of this report)<br>Unclassified | 20. Security Classif. (of this page)<br>Unclassified | 21. No. of Pages<br>50 | 22. Price |

**Form DOT F 1700.7** (8-72) Reproduction of completed page authorized
This form was electrically by Elite Federal Forms Inc.

# Feasibility Study of Scanning Laser System for Measuring Seal Coat Quality

**by**

*Richard Liu, Wei Sun, Wei Ren, Yuanhang Chen, Pankaj Chopra, Yu Cai, Jing Li, and Xuemin Chen*

**Research Report 0-5310-2**

Project Number: 0-5310
Project title: The Evaluation of a System for Measuring Seal Coat Quality

Performed in Cooperation with the
Texas Department of Transportation and Federal Highway Administration

by

Subsurface Sensing Laboratory
Department of Electrical and Computer Engineering
University of Houston

September 2007

## DISCLAIMERS

The contents of this report reflect the views of the authors, who are responsible for the facts and the accuracy of the data presented herein. The contents do not necessarily reflect the official view or policies of the Federal Highway Administration (FHWA) or the Texas Department of Transportation (TxDOT). This report does not constitute a standard, specification, or regulation.

University of Houston
4800 Calhoun Rd.
Houston, TX 77204

# ACKNOWLEDGMENTS

We greatly appreciate the financial support from the Texas Department of Transportation that made this project possible. The support of the project director and the project coordinator are also very much appreciated.

# Table of Contents

# List of Figures

# CHAPTER 1: INTRODUCTION

Seal coating is a common preventive maintenance activity in Texas highway system. It involves spraying asphalt cement on a surface of an existing pavement followed by application of a cover of aggregate.

The primary reason to seal coat is to prevent pavement from deteriorating by sun and rain. If only the asphalt itself is exposed under strong sun light, severe temperature change and heavy rainfall, the asphalt will harden, or oxidize. Thus it may lead to brittleness of the pavement and the pavement will also develop cracking as a result because it is unable to suffer from high traffic condition and sharp temperature changes. However, a seal coat can overcome these situations by providing a waterproof membrane which not only slows down the oxidation process but also helps improving pavement drainage, preventing water from infiltrating into base of pavement.

The other benefit of seal coating is increasing surface friction. The aggregates attached on the base of pavement will increase roughness of the pavement surface so that the overall surface friction can be increased by this way.

The problems emerge during new construction or during maintenance because the embedded depth of aggravates in the pavement asphalt surface is needed to be monitored and controlled in a relatively precise fashion. The criteria of differentiating the sealcoat quality can be obtained by precise measurement of surface mean profile depth (MPD) which is strongly related to the embedded depth of aggravates.

Different embedded depths are corresponding to different sealcoat conditions. The normal embedded depth must have to be approximately 70 percent of aggregate particles height into the residual asphalt, as shown in Fig. 1.

If the embedded depth is higher than the normal 70%, it is shelling (also called raveling). Shelling is a surface condition in which aggregates are lost from asphalt. Such pavements have a very irregular appearance since the surface is not completely covered by aggregates. This type of distress is generally observed on the centerline and between the wheel paths of the pavement. Shelling occurs when the desired bond between the aggregate and binder fails. Low binder application rates, inadequate rolling, cool weather construction, and incompatible binder and aggregate types are normal factors that might lead to shelling.

If the embedded depth is less than the normal 70%, the pavement surface is called flushing (also called bleeding). Flushing or bleeding is characterized by the excessive embedment of aggregate into the asphalt binder and a loss of skid resistance that is caused by the extra binder on the surface. In other words, a flushed surface has a smooth and slick appearance where the aggregates are less visible. Such distress is usually observed on the wheel paths where repetitive load cycle of tires cause subsequent embedment of aggregates. Flushing may be exacerbated by high binder application rates as well as with high surface temperatures during the day.

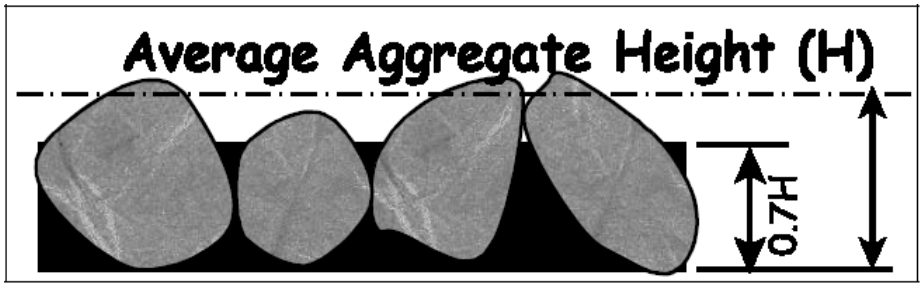


Fig 1.1 Proper embedment (~70%) into the residual asphalt

By far TxDOT spends as much as $180,000,000 to maintain 186,000 lane miles of roadway, and seal coats budget is a very significant part of overall TxDOT's preventive maintenance program budget. The primary tasks of this program are monitoring the highway pavement condition and updating Pavement Management Information System (PIMS) database frequently and efficiently.

The target of this project is to develop an algorithm and a device that can evaluate pavement condition and measure the MPD of the pavement in a highly efficient and accurate way. It is also important to make sure that all data measured by these devices can be compatible with PIMS data format and finally adopted by PIMS database.

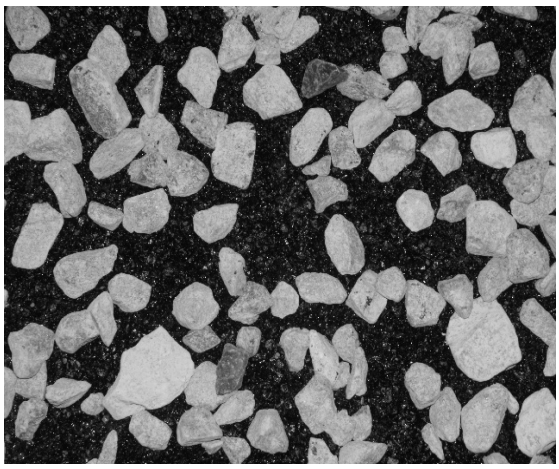

a)

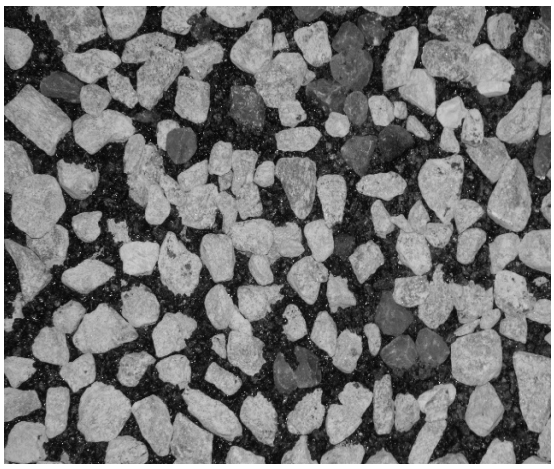

b)

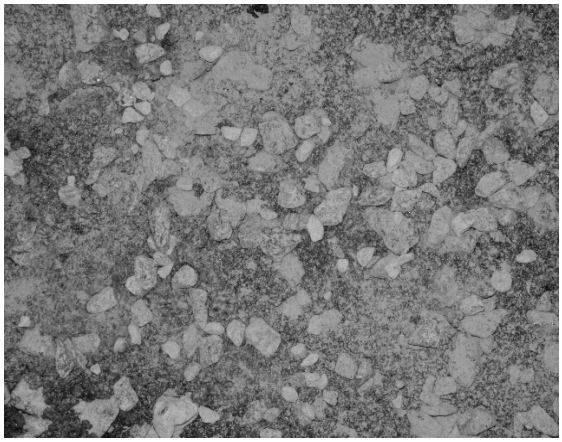

c)

Fig 1.2 Three typical pavement conditions

a) Shelled; b) Normal and c) Flushing.

Imaging method was attempted to solve this problem. However, due to the 2-Dimentional nature of the images, height information is not collected by the 2-D picture. Therefore, imaging method is not feasible to evaluate sealcoat quality. As a result, we decided to use high speed and high accuracy method based on laser distance measurement technology. In the following chapters, we will briefly discuss the development efforts and field test results.

# CHAPTER 2: HIGH SPEED TEXTURE LASER SYSTEM

## 2.1 Device Description

The Laser optical system (Fig 2.1 Fig 2.2) consists of three parts: a laser diode module, convex lens, and a position sensitive detector (PSD).

A laser diode module emits a laser beam to produce a light spot on the object surface. The convex lens collects part of the scattered light from the surface and converge it to an image spot on the PSD. If the distance between the measurement device and the object surface changes, the position of image spot on the PSD is also shifted. According to the position and the light intensity of the image spot, the PSD can output current signals to the electronic circuit. This is the basic principle of the laser triangulation optical subsystem.


Fig 2.1 Point Laser

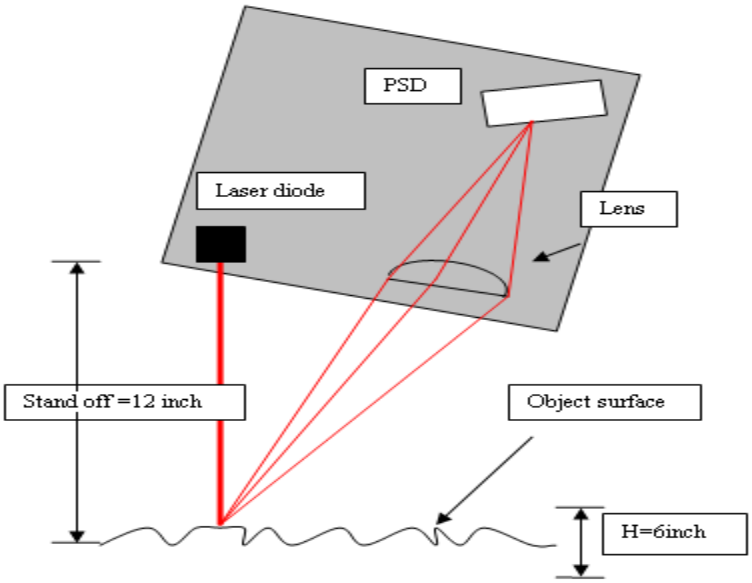


Fig 2.2 Point Laser Working Principle

**2.2 Specifications achieved from the device:**

- Standoff distance: 12 inches

The standoff distance means the distance between the laser source and object at which the output analog voltage from laser is approximately 0V.

- Measurement range: 6 inches (9 inches to 15 inches with 12 inch as stand off).
- Operating frequency : 154 KHz

The laser source is operated in the frequency range of 154 KHz.

- System clock: The device has a clock oscillator whose frequency is 1.54 MHz.
- Average power consumption: 0.75 A at 12V.The laser power supply board requires an input voltage of 12V.
- Peak to Peak voltage noise: about 80 -100 mV at a fixed distance of 12 inches.
- Wavelength of the laser diode : 785 nm ,75mW

- Voltage calibration curve (distance versus voltage) can be used to find out how much displacement with respect to change in voltage a laser device signifies.

## 2.3 Laser Calibration

Calibration of point laser is relatively simple. The calibration is just for converting voltage value to distance value. Although the range of the calibration curve beside standoff distance is almost linear, the rest of the curve is not a perfect linear. We use 6 orders polynomial to fit this calibration samples collected from calibration bench (Fig 2.3). Then an empirical equation can be got. (Fig 2.4) Any voltage value with unit of V (corresponding to x) can be put into that equation to get corresponding distance value with unit of mil (corresponding to y).

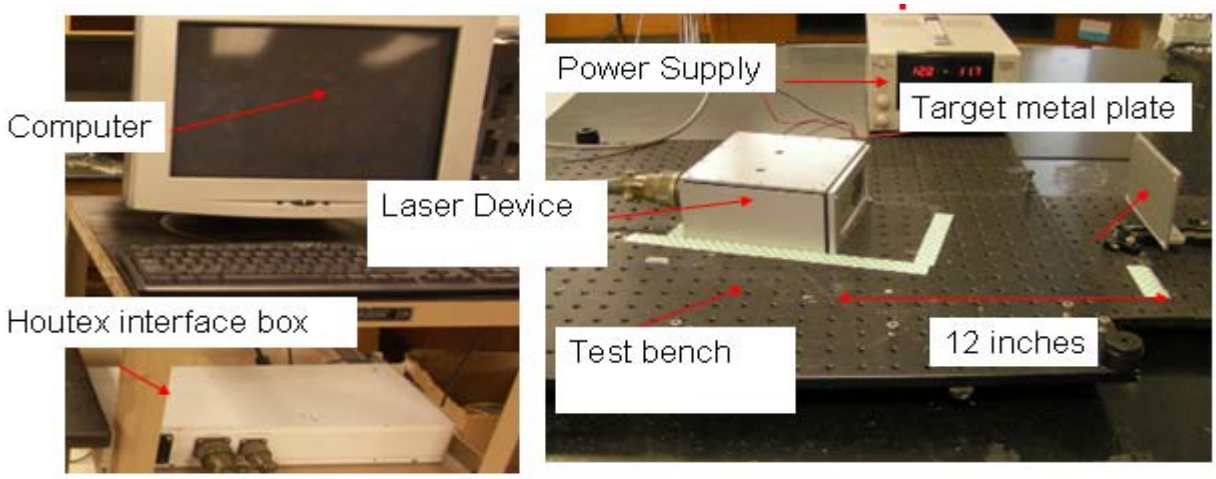


Fig 2.3 Calibration Bench

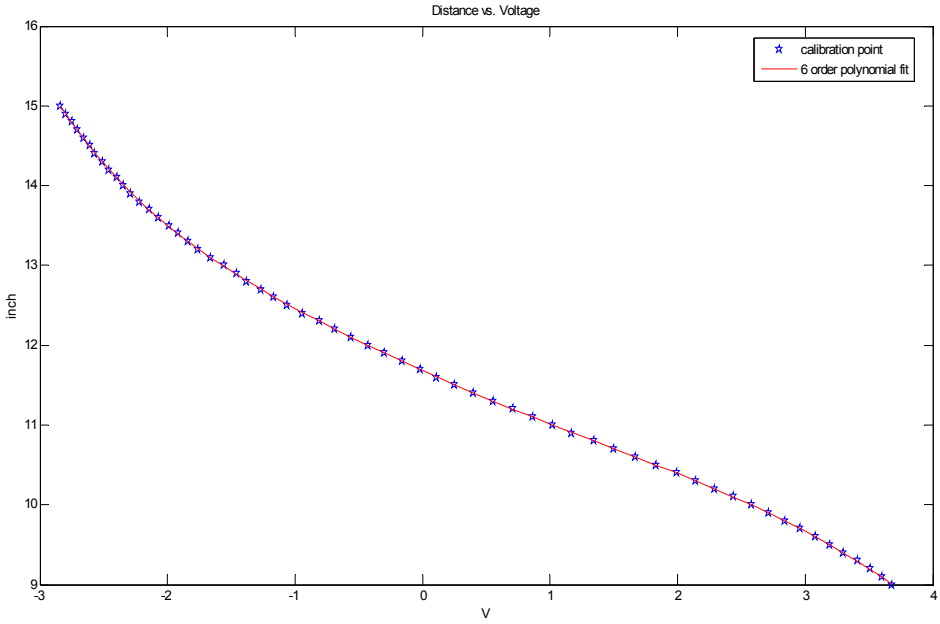


$$y = 0.003x^6 - 0.0023x^5 + 0.0022x^4 - 0.0059x^3 + 0.0531x^2 - 0.7161x + 11.6796$$

Fig 2.4 Calibration curve of Distance vs. Voltage and empirical equation

# CHAPTER 3: SCANNING LASER SYSTEM

## 3.1 Principle Review of laser Triangulation

The triangulation method (Manuel 1996, Wiese 1989) is the most commonly used approach in modern industry for applications requiring an operating range that is less than 10 meters. Currently, there are a limited number of triangulation-based sensors available commercially for the ranges between 2 meters and 10 meters. The fundamental geometrical principle of optical triangulation is shown in Fig 3.1. Fig 3.2 shows the basic geometrical principle of laser scanning triangulation. The laser beam is deflected by a scanning mirror and scans over the object. A camera, constituted of lens and a position sensitive photodetector, measures the location of the image of the illuminated point on the object.

The laser-optical triangulation has been widely used in many applications of both profiling and range measurement for its advantages of low cost, simplicity, robustness and good resolution. Although having those advantages, the classical triangulation technique has some limitations.

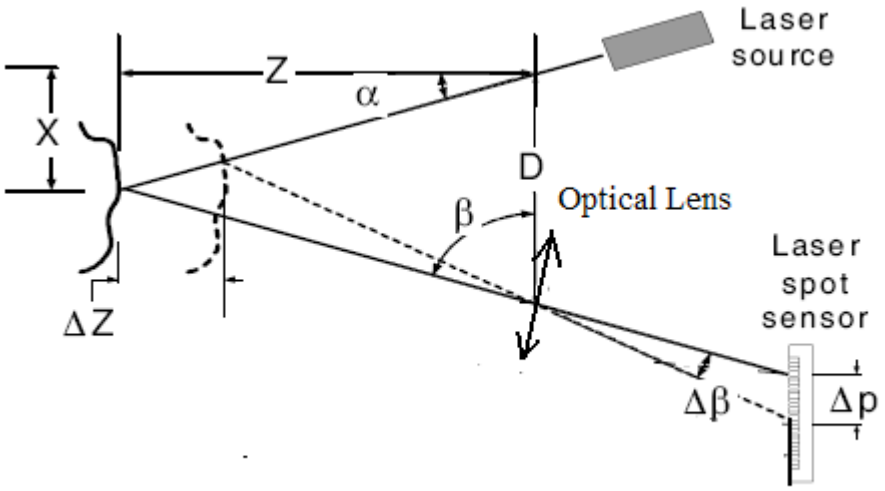


Fig 3.1 Geometrical Principle of Triangulation

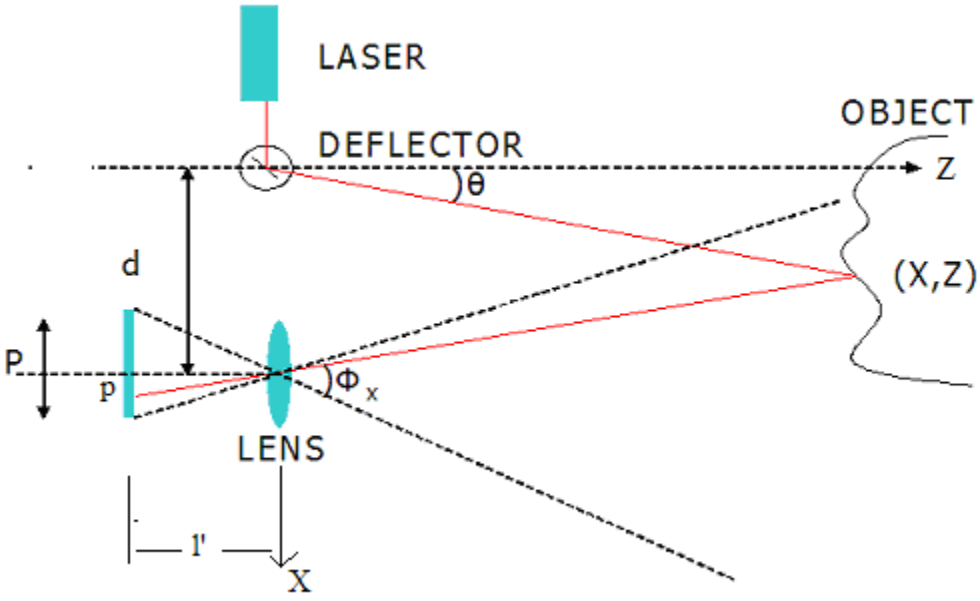


Fig 3.2 Geometrical Principle of Laser Scanning Triangulation

To alleviate the problems associated with the classical triangulation, an innovative approach called auto-synchronized scanning mechanism that allows a very large field of view without compromising the performance of the system is introduced.

## 3.2 Auto-Synchronized Laser Scanning Principle

### 3.2.1 Optical configuration of auto-synchronized scanning laser principle

The innovative approach of auto-synchronized scanning technique was presented (Rioux 1994). The basic idea is to synchronize the projection of a light spot with its detection. Fig 3.3 shows the optical configuration of the auto-synchronized scanning laser system. A double-sided coated mirror is used as a scanning device. One side of the mirror is used to deflect the laser beam. The other side collects the reflected light from the scene. By using this configuration, the instantaneous field of view follows the laser spot as it scans over the scene, which means the focal length of lens f is therefore related only to the desired depth of field or measurement range.

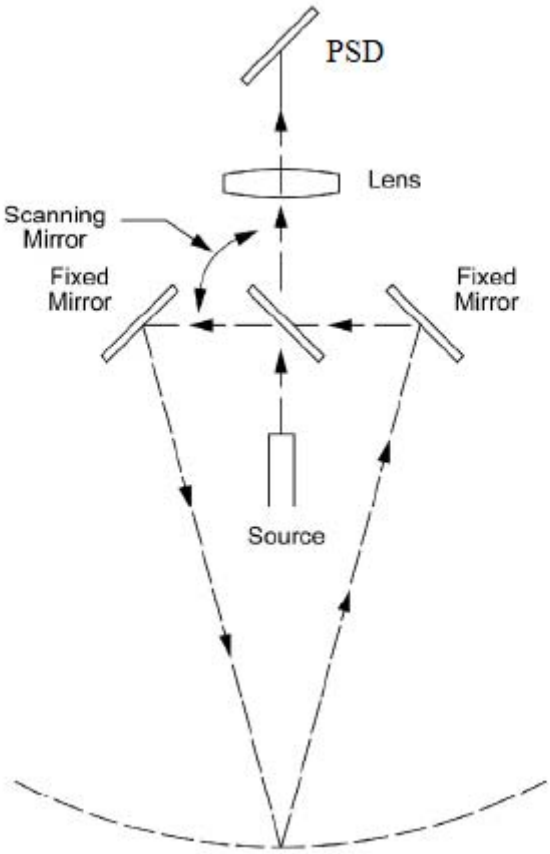


Fig 3.3 Optical Configuration of Auto-Synchronized Laser Scanning

### 3.3 Device Description

The developed auto-synchronized scanning laser device is shown in Figure 2-6.

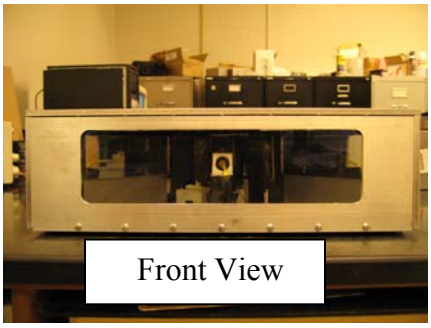


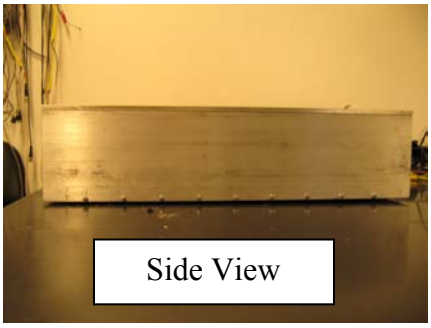


Fig 3.4 Laser Device Based on Auto-synchronized Scanning Principle

The physical dimensions of the laser device are 16.248 inches width, 20.185 inches depth and 4.724 inches height.

The internal structure of the scanning laser device is shown in Fig 3.5. The device consists of a laser diode, scanning mirror, projection mirror, recollection mirror, lens, position sensitive detector, signal processing circuitry and power supply.

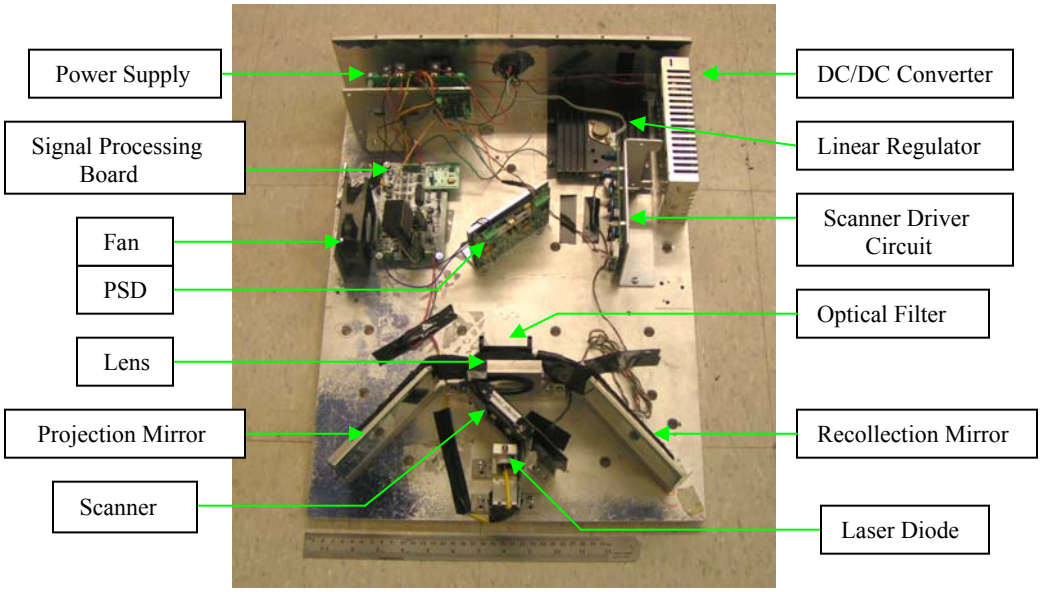


Fig 3.5 Internal Structure of the Scanning Laser Device

To descript the architecture of the device, a simple hardware block diagram is depicted in Figure 3.6.

The prototype hardware of the pavement marking thickness measurement system based on the auto-synchronize laser scanning technique is composed of a laser optical subsystem, electronic processing and control subsystem, and power supply subsystem. The laser optical subsystem has been described before. The electronic processing and control subsystem consists of a laser signal processing circuit, scanning driver circuit and data acquisition. Only a 12 V DC power supply is necessary for the device. By using DC-DC voltage converters and voltage regulators, the 12 V output from the DC power supply is converted to + 15 V and +5 V, which is necessary for the laser electronic signal processing circuit.

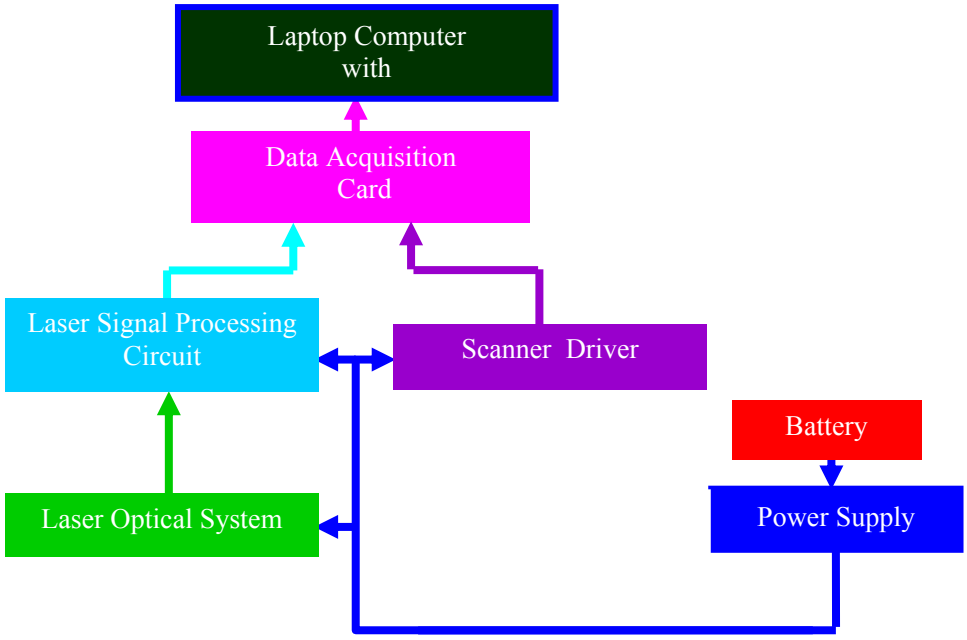


Fig 3.6 Block Diagram of Hardware

# CHAPTER 4: LAB RESULTS

## 4.1 Scanning laser setup in the Lab

To verify the accuracy the developed device, three asphalt samples have been built, a bare, a medium, and a flushed sample, as shown in Fig 4.1.

Fig 4.1 Test Samples of Bare, Medium, and Flushed Asphalt Slabs

To verify the device, the scanning laser device and the sample slabs are installed as shown in Fig 4.2. The distance between the front window of the device to the sample slabs is 93 cm. The raw data is shown in Fig 4.3, from which it can be seen that the developed scanning laser device is able to tell the difference of the flushed, medium, and bare asphalt samples.

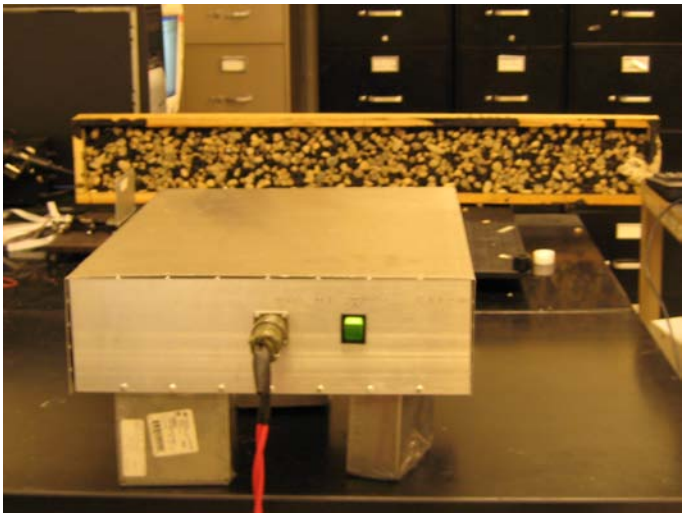

Fig 4.2 Installation of the Scanning Laser Device and the Sample Slabs

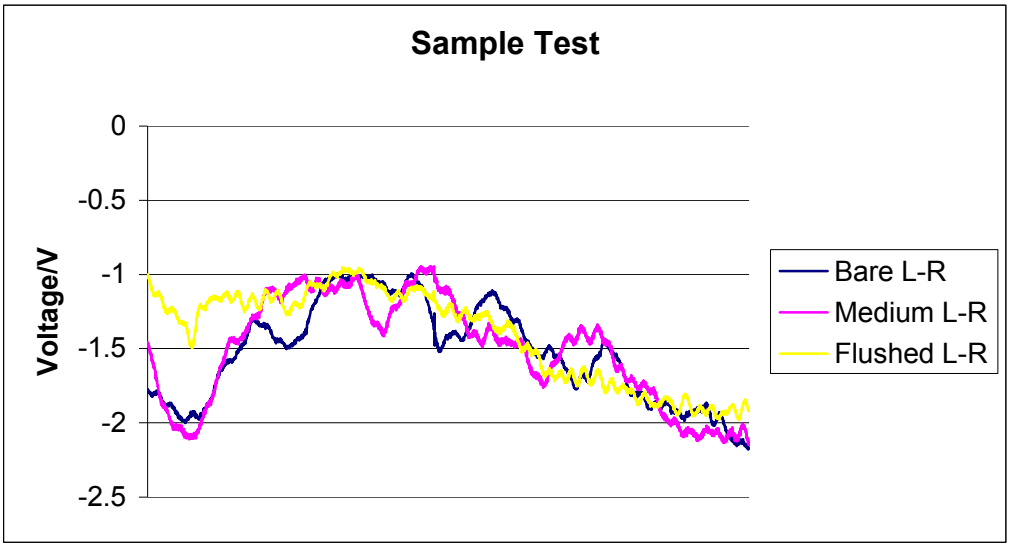


Fig 4.3 The raw data of the sample test, which proves that the device is able to tell the differences of the flushed, medium, and bare asphalt samples

### 4.2 Calibration Using Calibration Plate

Calibration is one of the most important issues among all the scanning laser data processing problems. In this section, the calibration is in a sense that converting original raw parabolic or any other irregular curve from scanning laser into straight line, which is different from the MPD calculation calibration process in the Chapter 5~6.

We developed an algorithm that can convert an empirical equation for converting these parabolic curve or humps to straight line sets.

To calibrate the device and make the calibration curves for signal processing, a computer-controlled mechanical bench is used, shown in Fig 4.4, which can move the target along Y direction accurately. A calibrate plate is used as the target as shown in Fig 4.5.

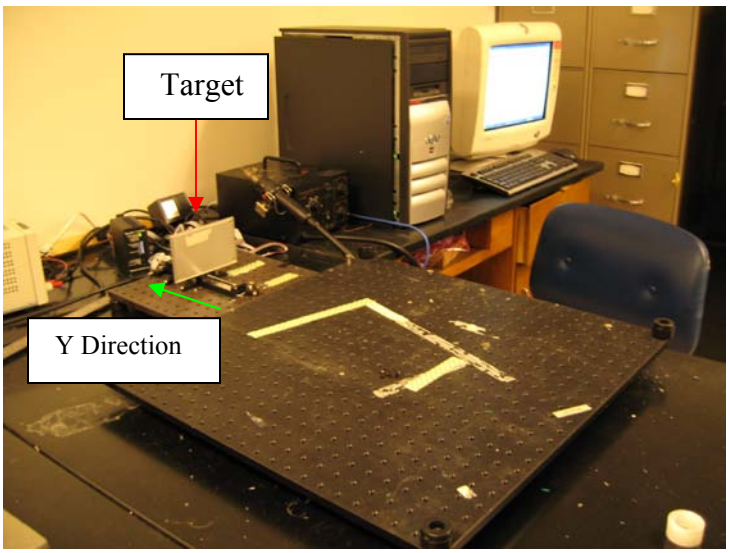


Fig 4.4 Computer-Controlled Mechanical Bench.
(The target can be moved along the Y direction accurately.)

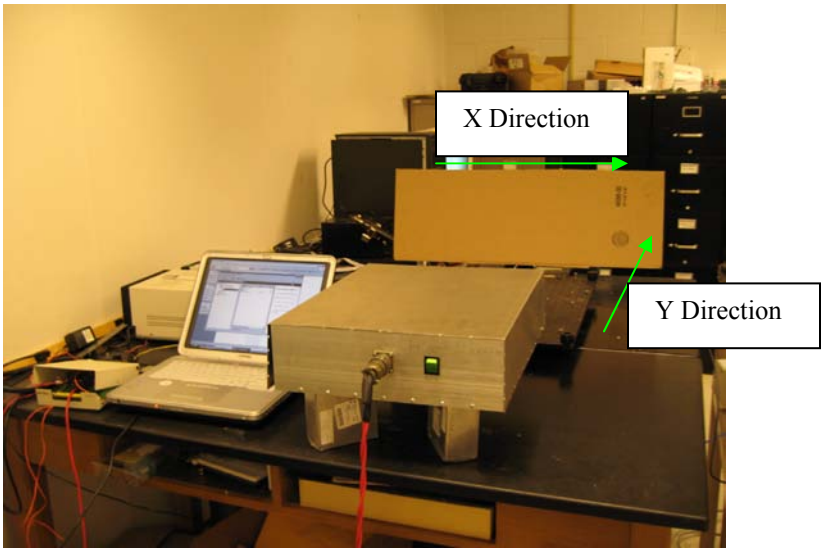


Fig 4.5 Scanning laser calibration test setup. A paper board is used as the target. The range of the distance from the front windows of the scanning laser device to the target is from 35.375 inches to 38.375 inches.

The target plate is moved along Y direction every 0.1 inch from 35.375 inches to 38.375 inches to generate 31 calibration curves. Fig 4.6 shows the raw data of these 31 calibration curves. Fig 4.7 shows the calibration curves after been processed by calibration software designed by ourselves. From these 2 figures we can see that the resolution along the Y direction is pretty good, below 1 mm. After that we transform the sinusoidal-wave curves into the flat curves and finish the calibration, which is shown in Figure 4.6-4.8.

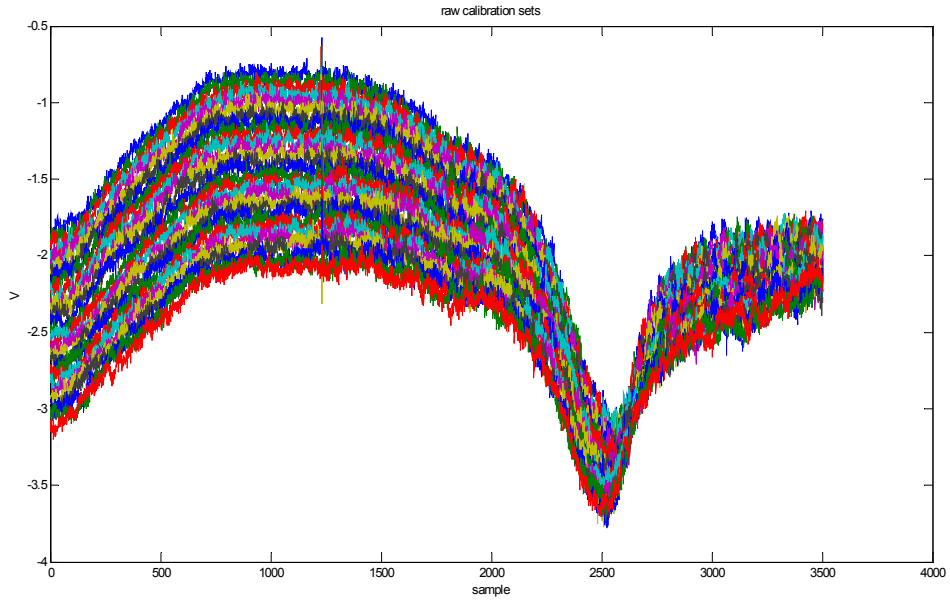


Fig 4.6 The raw data of the calibration curves

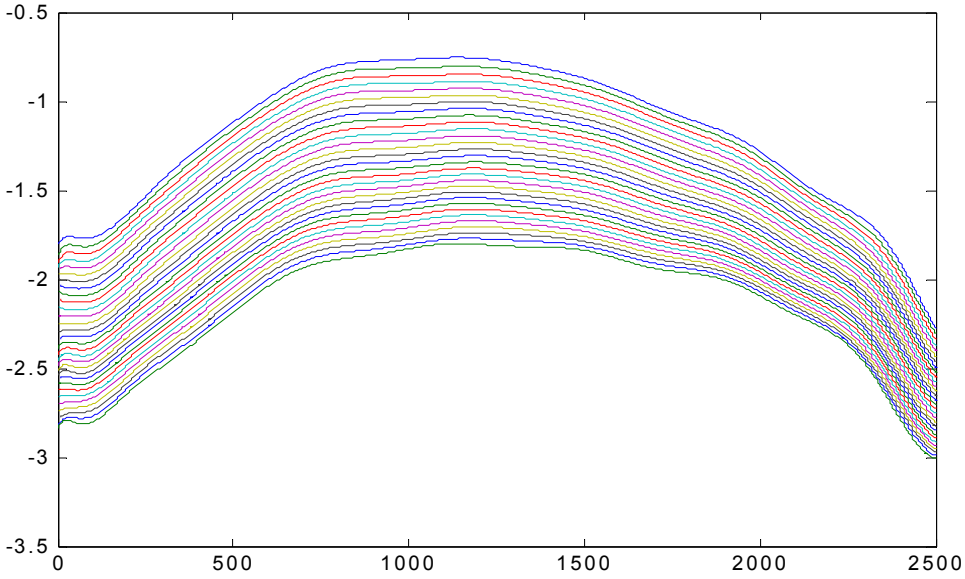


Fig 4.7 The parabolic calibration curves after processed by the software developed by SSL

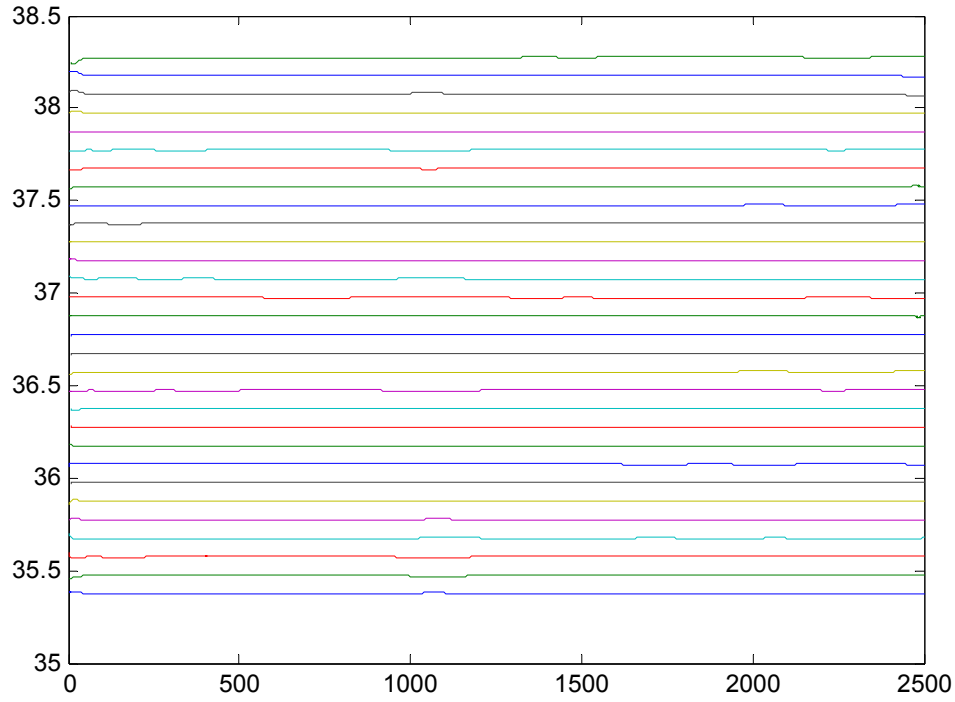


Fig 4.8 The final flat calibration curves we used for calibration.

After previous calibration process and data collection, we use a table mapping method to map the parabolic curve sets to straight line sets by using polynomial fit method to overcome the discrete sampling effects. In the other word, we got a discrete 2 D calibration matrix and then using polynomial interpolation method to get a 2 D continuous mapping matrix then we can easily convert any measured curve which is inside the parabolic curve sets area to a real profile curve.

This algorithm is implemented in MATLAB and is also easy to transplant to C code or to be embedded into any real-time system.

# CHAPTER 5: MPD CALCULATION ALGORITHMS

Mean Profile Depth is the most important parameter that is used to evaluate pavement condition. The algorithm of MPD calculation is detailed in ASTM E1845-01 standard.

## 5.1 ASTM Standard

MPD calculation method given in the ASTM is suitable for the calculation of the average macrotexture depth from profile data. The results of this calculation (MPD) have proven to be useful in the prediction of the speed dependence of wet pavement friction.

For MPD calculation, minimum requirements are ten evenly spaced profiles of 100mm (3.9 in.) in length for each 100 m (3900 in.) of the test section. However, for a uniform test section, it is sufficient to obtain 16 evenly spaced profiles regardless of test section length.

Data processing is the key of ASTM standard. It defines the principles and base to MPD calculation software. It consists of 7 parts which are Outliers, Lowpass Filtering, Segmenting the Profile, Slope Suppression, Peak Determination, Determination of MPD and Calculation of ETD. The details of MPD computation requirements can be found in ASTM standard E 1845 – 01: Standard Practice for Calculating Pavement Macrotexture Mean Profile Depth.

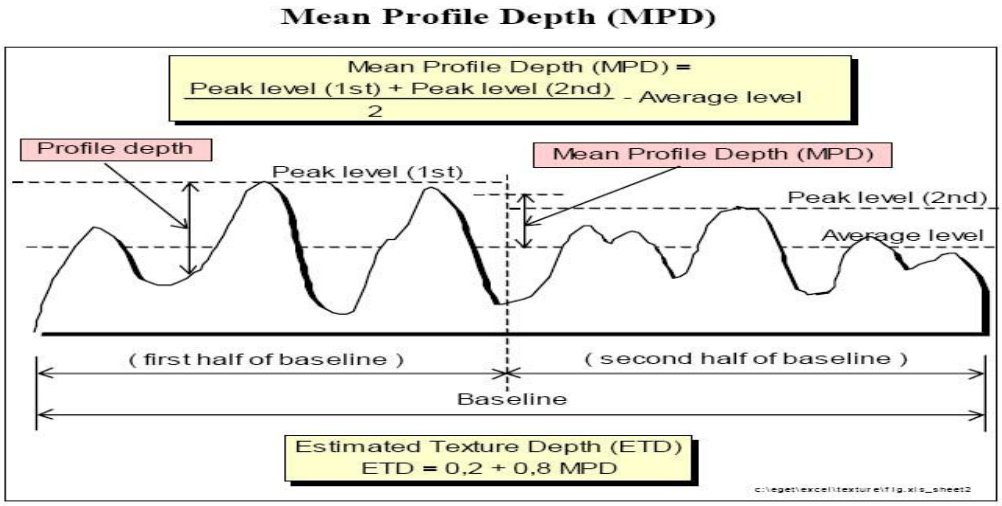


Fig 5.1 MPD definition

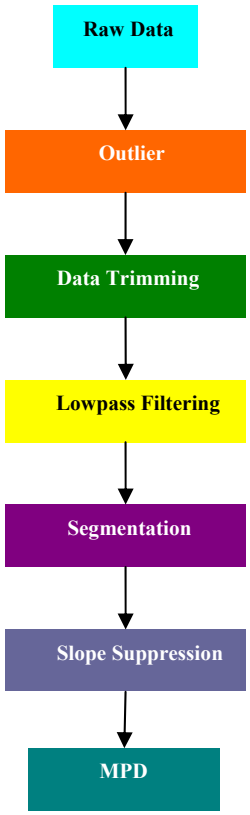


Fig 5.2a MPD calculation flow chart

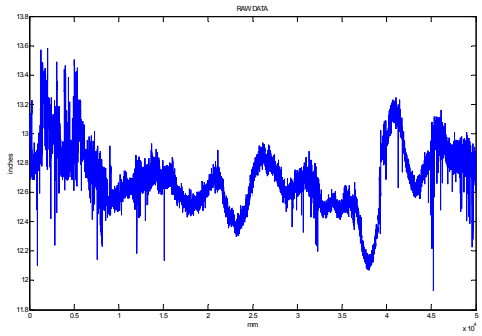
RAW DATA
inches
mm
x 10^4

a)

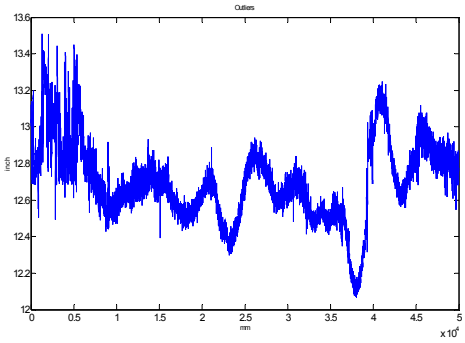
Outlies
inch
mm
x 10^4

b)

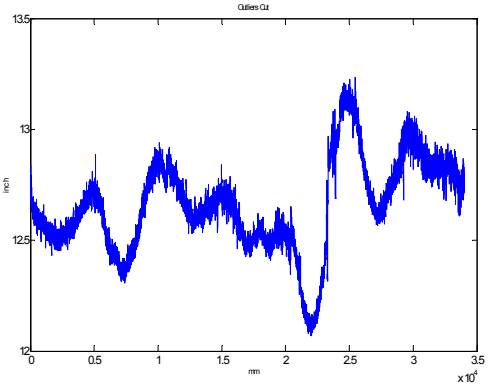
Outliers Cut
inch
mm
x 10^4

c)

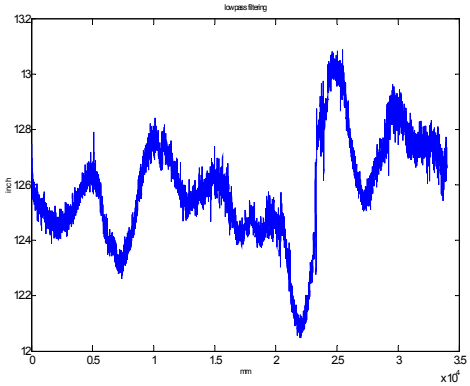
lowpass filtering
inch
mm
x 10^4

d)

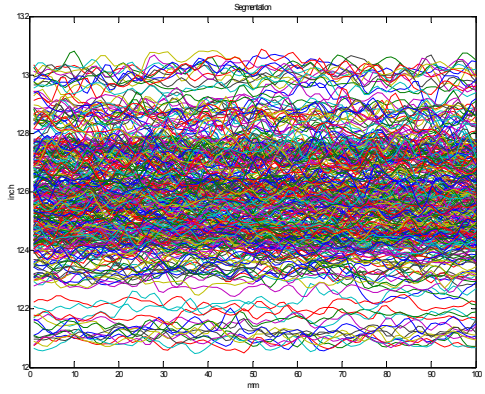
Segmentation
inch
mm

e)

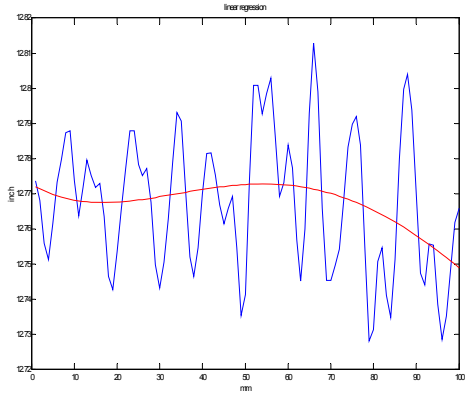
linear regression
inch
mm

f)

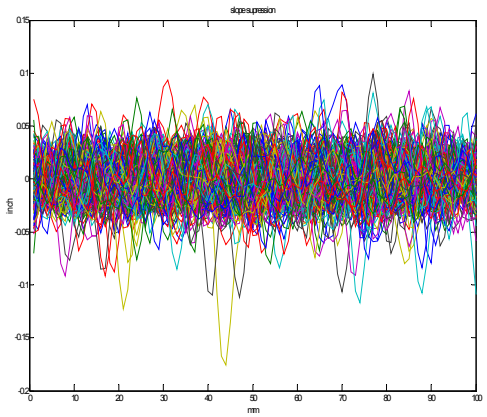


g)

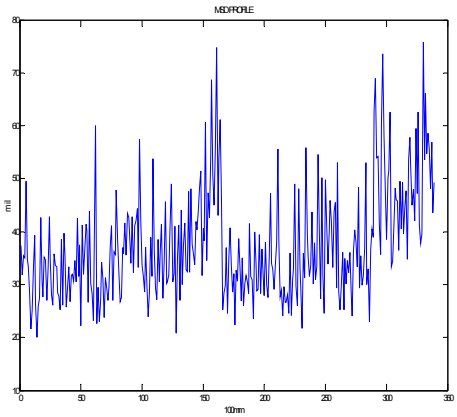


i)

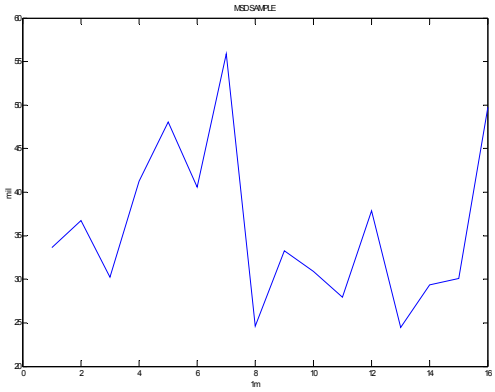


j)

Fig 5.2b MPD data processing procedures. a) raw data; b) outlier; c)outlier cut; d) lowpass filtering; e) segmentation; f) one sample of slope suppression; g) slope suppression; j) mean segment depth.

Figure 5.2a is a block diagram of the MPD computation . To illustrate the process of MPD computation, an example of MPD computation is shown. Fig 5.2b shows steps of data processing for calculating MPD. Here a) is the raw data, and b) outliers which remove some points that are out of reasonable range. c) data trimming to obtain useful data section from raw data; d) lowpass filtering of high frequency texture information; e) slope suppression to remove influence from slow changing slopes and to make sure the average value of the data is zero; f) mean segment depth profile, the overall MPD is

calculated from mean value of the evenly spaced 16 samples from this mean segment depth profile.

# CHAPTER 6: FIELD TEST

## 6.1 MPD Measured by point laser

As shown in previous chapters, point laser is a high resolution distance detector. When vehicle in which the laser mounts doesn't move, it's a one point distance detector. When the vehicle drives along the highway, it becomes a 1-D profiler or texture measurement device.

Because point laser is with very high vertical sensitivity and resolution, it is can be used to obtain accurate and repetitive MPD measurement. In this section, a set of field test results will show how the overall performance of this device is in practical environment.

We selected a couple of typical sites in Houston area to test point laser with its MPD calculation software. The test sites consists of Texas state highway 288 (Shelled), Old Spanish/Texas state highway 90 (normal)

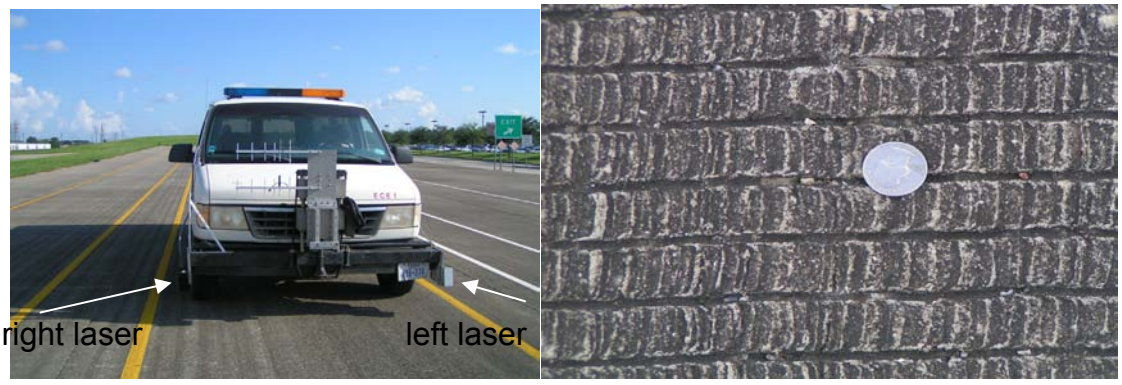


a) b)

c) d)

Fig 6.1 Test sites in Houston Area a) test sites in Texas Spur 5; b) Spur 5 pavement condition; c) SH 288 pavement condition; d) SH 90 pavement condition.

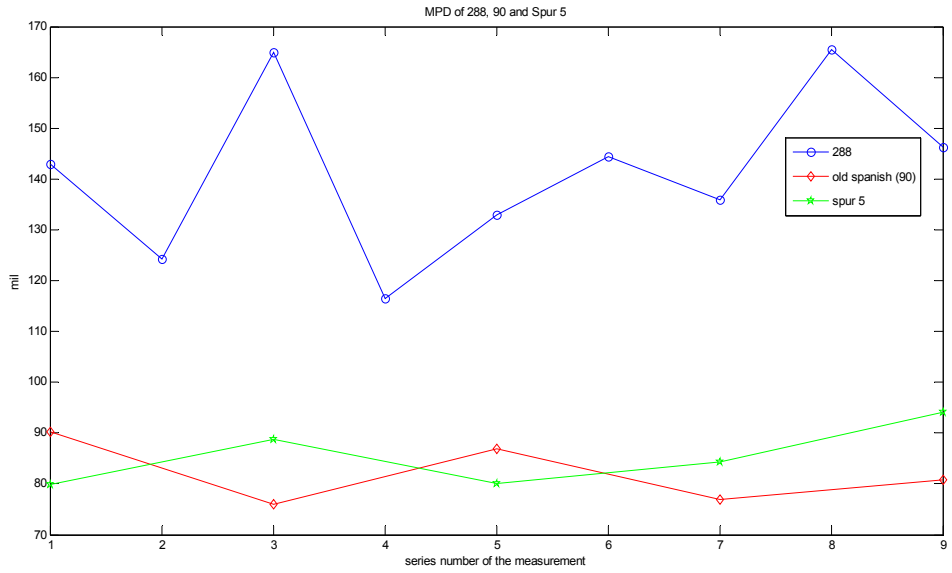


Fig 6.2 Point Laser testing results in SH 288, 90 and Spur 5

Fig 6.1 shows the pavement conditions of testing sites in Houston areas. Fig 6.2 is the data collected by the point laser. It shows the point laser is repetitive and it can difference of MPD value between shelled ( > 120 mils) and normal (around 95 mils) pavement condition is very significant. The more details and discussion over relations between MPD and pavement condition will be detailed in the following sections.

## 6.2 MPD Measured by scanning laser

When the van is moving, the scanning trace of the scanning laser device is zig-zag line, shown in Fig 6.3. Since the scanning rate is 50 Hz, when the van is driving at the speed of 30 MPH, the distance between each period line along the driving direction is 13.3 cm. To calculate MPD, the distance between each sample point should be less than 1 mm, so this scanning laser device can only calculate the MPD along the direction shown in the figure.

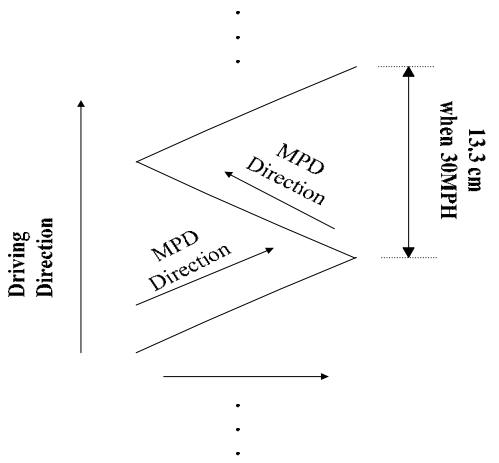


Fig 6.3 MPD direction of the scanning laser device

It is noted that the driving speed here is not necessarily to be 30mph for calculating the MPD along the zig-zag line. The speed can be up to 70mph. However, if a real 3-D MPD needed to be calculated, the laser's scanning speed needs to be increased otherwise the MPD calculation along the driving direction is impossible. That's a topic for future research and development for higher speed scanning laser.

### 6.3 Field Test in San Antonio

There are a few test sections in San Antonio area were selected as field test site. The idea was to use both laser devices and measure MPD. In the same site, use CMT and outflow meter to measure MPD and compare the data from these independent devices.

We selected 2 sections on FM-1376 in San Antonio, one is shelled section and the other is flushed section. On each section, 5 repetitive tests were run. Fig 6.4 shows the field tests and MPD results of the shelled section. The MPD measured by CMT is used as reference. CMT shows a MPD of 2.5 ~ 2.7 mm on this section, or 98.4 ~ 106 mils.

**(a)**

**(b)**

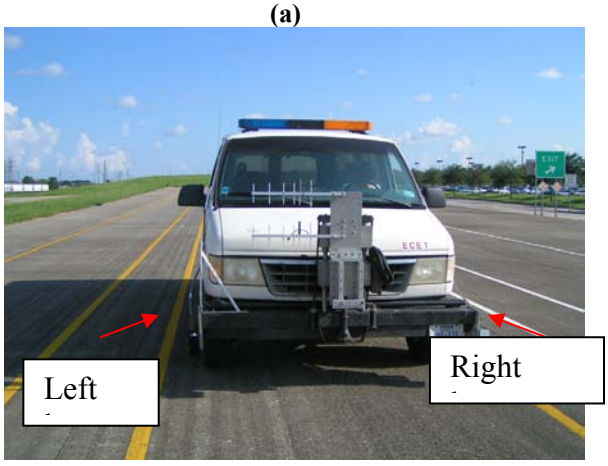


(c)

Fig 6.4 MPD measurement with point laser in FM1376. (a) Picture of the road surface; (b) CMT Test to get the reference MPD value, 98.4 ~ 106 mils; (c) Point laser device under test.

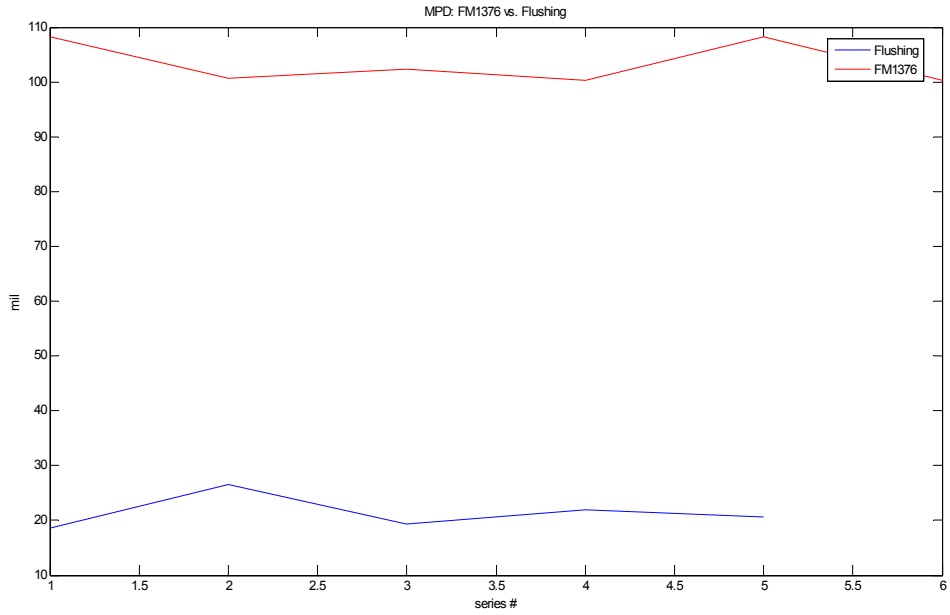


Fig 6.5 MPD comparison of the point laser device in flushing and shelled section.

Fig 6.5 shows MPD value of point laser is very repetitive and variance of MPD for 5 consecutive times is small (<+/-10mil). The shelled MPD calculated by point laser device, which is around 100 ~ 109 mils. Flushing MPD is about 20mils.

Fig 6.6 shows the field test of scanning laser in the flushed section of FM-1376 in San Antonio. The reference MPD calculated by Outflow-Meter Test is 20 mils. The flushing MPD calculated by the scanning device is around 20 ~ 40 mils. The shelled MPD from scanning laser is around 90mils. The variance of MPD calculated from the scanning laser is bigger than point lasers although the difference between shelled and flushing is significant (Fig 6.7).

(a)

(b)


(c)

Fig 6.6 MPD Test with scanning laser in FM1376. (a) Picture of the road surface;
(b) Outflow-Meter Test to get the reference MPD value, 20 mils;
(c) Scanning laser device under test

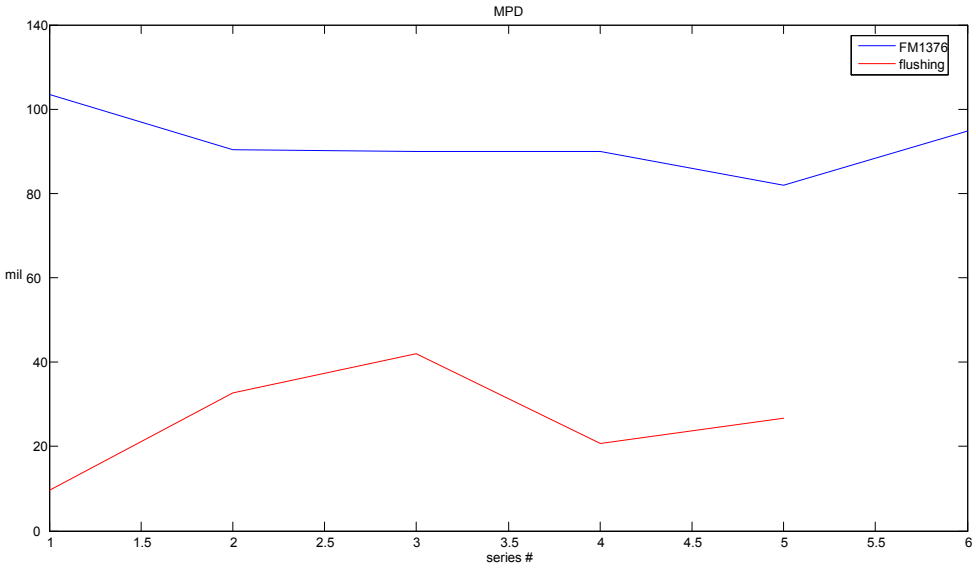


Fig 6.7 MPD comparison of the scanning laser device in flushing and shelled sections.

### 6.3 Performance comparison between scanning laser and point laser

In order to compare results from both laser devices, careful calibration must be conducted. Before hardware calibration, the most important issue is that we have to make sure that the test result should be repetitive if the measurement is under that same condition. In another word, if we test the same section for a few times, we have to make sure that the MPD calculated from our software should be in a given range and the variance should not be greater than +/- 10mil.

If the results meet these variance requirements, we can conclude that the device is working properly and initiate calibration process.

The calibration reference data are from CMT data or Out-flow meter data. It is found that scanning laser normally measures higher MPD value than point laser. Since laser data from both devices are very repeatable, it is easy to generate a calibration table which can map the raw data to actual surface roughness data. In the field application, these mapping tables will be kept for each device and the calibration coefficients are embedded into the processing software to calibrate measurement results.

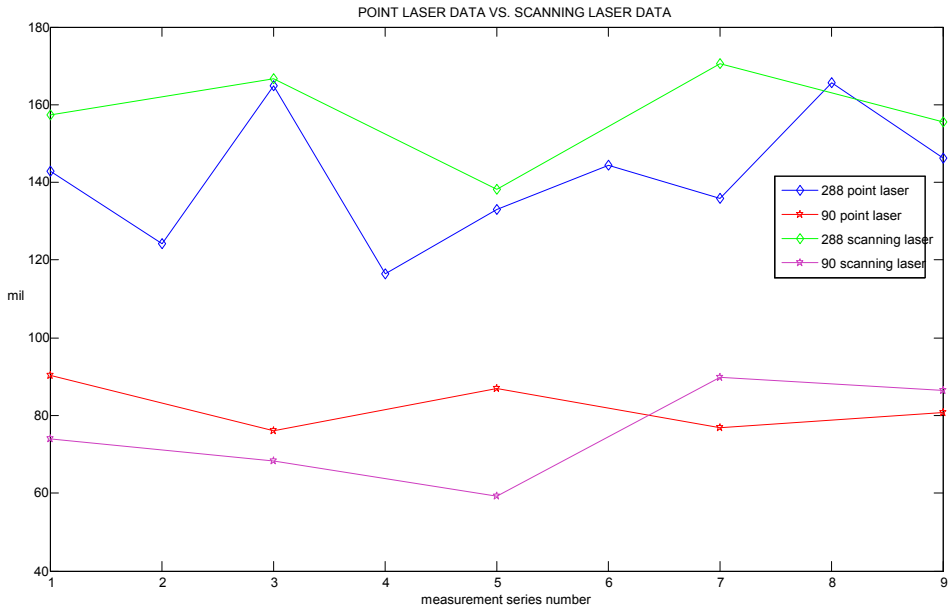


Fig 6.8 Point Laser Data vs. Scanning Laser Data

(Shelled and normal condition)

The point laser's performance was compared with scanning lasers' in shelled (288) and normal (90) sections. In these cases, their performance is with no big difference. The variance of 288 data is big because it's with different sections on 288.

## 6.4 Low, Medium and High Flushing sections

In order to better understanding to the relationship between MPD and pavement characteristics, a set of data collected from Conroe, TX are analyzed. As shown in Fig 6.10, Green color sections correspond to low flushing. Yellow sections are with medium flushing and red sections are with high flushing sections.

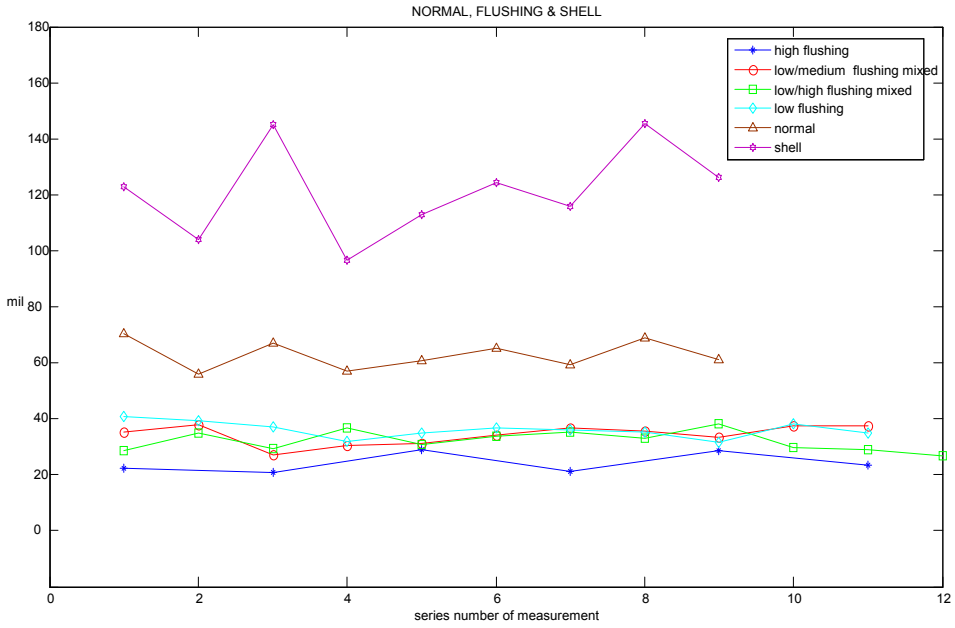


Fig 6.9 MPD by Point Laser in high, medium, low flushing section and normal, shelled section

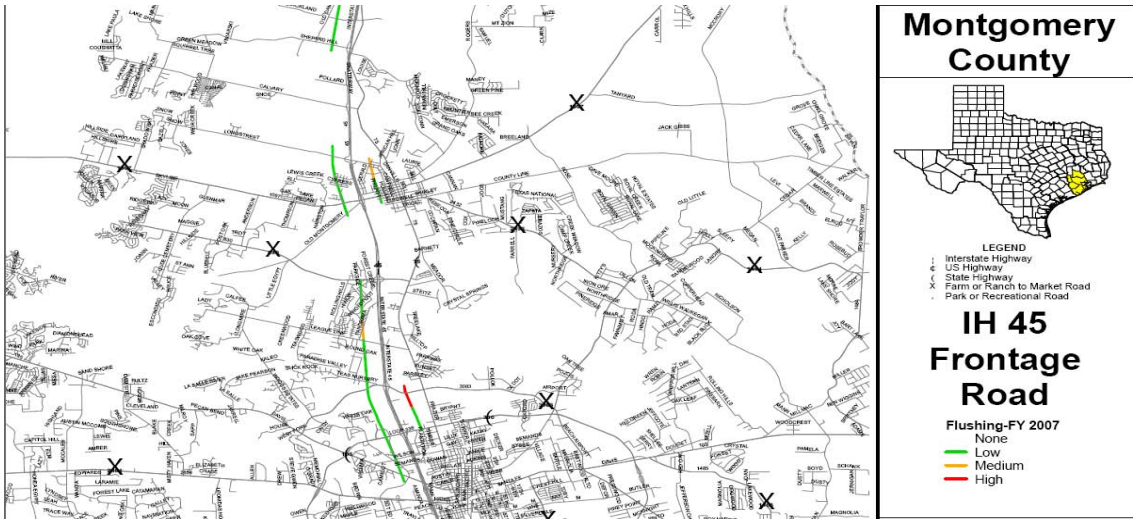


Fig 6.10 Test Sites of Fig 6.6 in Conroe, TX.

The difference between high flushing, medium flushing or low flushing is difficult to detect with the MPD value measured by the lasers. (Fig 6.9) The MPD curves with medium, low or high flushing pavement are intertwining with each other. The gaps between normal, flushing and shelled are significant.

### 6.5 MPD criteria

Based on all the field test data and previous discussions and post data processing, criteria for evaluating sealcoat quality is established for the laser devices. Table 6.1 shows these criteria. These criteria can be used for both point laser and scanning laser devices. Figure 6.11 shows these criteria graphically.

**Table 6-1 Criteria evaluating sealcoat quality using laser devices**

| Pavement | MPD Range(mils) |
|---|---|
| Shelled | >95 |
| Normal | 40~95 |
| Flushed | <40 |

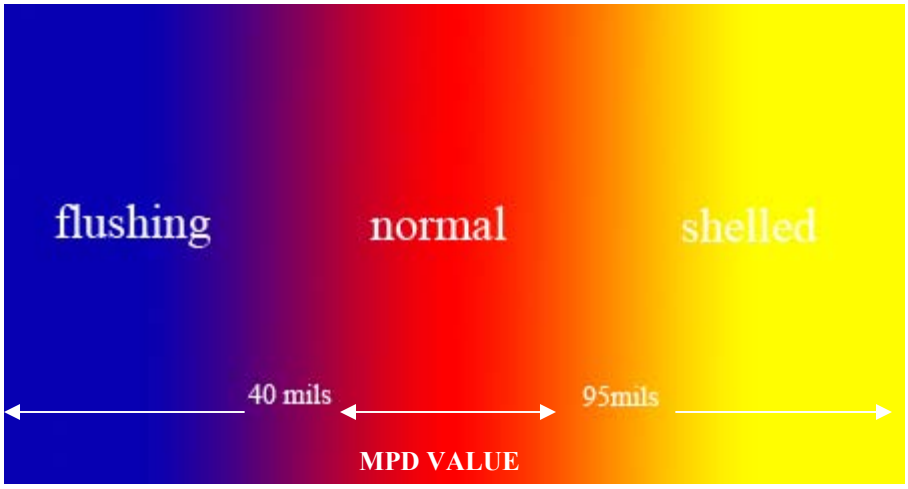


Figure 6.11 Criteria evaluating sealcoat quality using laser devices

# CHAPTER 7: CONCLUSIONS AND SUGGESTIONS

In this project the researchers developed a methodology, two hardware systems, and software to evaluate sealcoat quality at highway speed. The methodology is based on mean profile depth (MPD) measured by high speed laser devices. The two hardware systems are texture laser device and scanning laser device. A high-speed texture laser and a 3-D scanning laser system based on auto-synchronized scanning technology are developed in this project. A mean profile depth algorithm based on ASTM standard has been developed and embedded into both point laser and scanning laser devices. The two different devices are mounted on a measurement van and field-tested in pavement sections in San Antonio, Texas. The results of these devices are compared with the MPD value measured by outflow meter. The results are proved to be accurate and can be used in a high-speed measurement in harsh environment. A criterion of automatically identifying a pavement section for flushing, shelling or normal surface conditions is also developed using the field data from both devices.

Recommendations to TxDOT include the following:

1. Non-contact, high speed devices based on laser technology is feasible to evaluate sealcoat quality at highway speed;
2. Both point laser and scanning laser are useful for obtaining raw sealcoat quality information;
3. Point laser system has higher accuracy than scanning laser system;
4. MPD can be used as indicator of sealcoat quality;
5. Implementation of this project should be considered.

## References:


Benson, F.J. and Galloway, B.M. (1953) Retention of Cover Stone by Asphalt Surface Treatments, Bulletin 133, Texas Engineering Experiment Station, Texas A&M University System.

Blais F., Rioux M., Beraldin J-A. (1988) Practical considerations for a design of a high precision 3-D laser scanner system, *Proc of the SPIE.*, Vol. 959, pp 225-246.

Brock, J. D., May, J. G., and Renegar, G., *Segregation Causes and Cure*s. *Technical Paper T-117*, Astec Industries, Chattanooga, Tenn., 1996.

Dremel, W., Häulser, G., and Maul M.(1996) Triangulation with a large dynamical range. *Proc. SPIE.,* 665, 182-187.

Holmgreen, R.J., Epps, J.A., Hughes, C.H. and Galloway, B.M. (1985) Field evaluation of the texas seal coat design method, Research Report 297-1F, Texas Transportation Institute, Texas A&M University System, College Station.

Janisch, D.W., and F.S. Gaillard. (1998). *Minnesota Seal Coat Handbook* . Report MN/RC-1999-07. Minnesota Local Road Research Board, Minnesota Department of Transportation, St. Paul, MN.

Manuel, C. F. M. (1996) Surface Inspection by an Optical Triangulation Method, *Opt. Eng*., 35(9), pp. 2743-2747.

Nicholas J. G., and Lester A. H., (1997). *Traffic and Highway Engineering*, 2nd Ed., PWS Publishing Co., New York.

Roadware Corporation, "Technical Reference Manual - Version 1.1," 1995.

Rioux, M. (1994) Laser range finder based on synchronized scanners, *Appl. Opt*., 23(21), pp. 3837-3844.

Rioux, M., and Bechtold, G., Taylor, D., and Duggan, M., (1987). Design of a large depth of view three-dimensional camera for robot vision, *Opt Eng.,* 26(12), pp. 1245-1250.

Wiese, D. R., (1989) Laser Triangulation Sensors: A Good Choice for High Speed Inspection, *Chilton's I&CS (Instrumentation and Control System)*, 62, pp, 27-29.